# A global assessment of the impact of school closure in reducing COVID-19 spread

**Joseph T. Wu** (joewu@hku.hk)
The University of Hong Kong https://orcid.org/0000-0002-3155-5987
**Shujiang Mei**
Shenzhen Center for Disease Control and Prevention
**Sihui Luo**
University of Science and Technology of China
**Kathy Leung**
University of Hong Kong
**Di Liu**
University of Hong Kong
**Qiuying Lv**
Shenzhen Center for Disease Control and Prevention
**Jian Liu**
Anqing Hospital Affiliated to Anhui Medical University
**Yuan Li**
Shenzhen Center for Disease Control and Prevention
**Jianping Weng**
University of Science and Technology of China
**Tiejian Feng**
Shenzhen Center for Disease Control and Prevention
**Xueying Zheng**
University of Science and Technology of China
**Gabriel M Leung**
The University of Hong Kong https://orcid.org/0000-0002-2503-6283

**Research Article**

**Keywords:** COVID-19, school closure, control intervention, effectiveness

**Posted Date:** August 6th, 2020

**DOI:** https://doi.org/10.21203/rs.3.rs-53593/v1

**Version of Record:** A version of this preprint was published at Philosophical Transactions of the Royal Society A: Mathematical, Physical and Engineering Sciences on November 22nd, 2021. See the published version at https://doi.org/10.1098/rsta.2021.0124.

**A global assessment of the impact of school closure in reducing COVID-19 spread**

Joseph T Wu[1*], Shujiang Mei[2*], Sihui Luo[3,4*], Kathy Leung[1*], Di Liu[1], Qiuying Lv[2], Jian Liu[5], Yuan Li[2], Jianping Weng[3,4], Tiejian Feng[2#], Xueying Zheng[3.4#], Gabriel M Leung[1#]

[1] WHO Collaborating Centre for Infectious Disease Epidemiology and Control, School of Public Health, LKS Faculty of Medicine, The University of Hong Kong, Hong Kong SAR, China

[2] Department of Communicable Diseases Control and Prevention, Shenzhen Center for Disease Control and Prevention, Shenzhen 518055, China

[3] The First Affiliated Hospital of USTC, Division of Life Science and Medicine, University of Science and Technology of China, Hefei, China

[4] Clinical Research Hospital (Hefei) of Chinese Academy of Science, Hefei, China

[5] Anqing Hospital Affiliated to Anhui Medical University (Anqing Municipal Hospital), Anqing, China

[*]These authors contributed equally as co-first authors

[#]These authors contributed equally as co-senior authors

Corresponding author: Joseph T. Wu, School of Public Health, LKS Faculty of Medicine, The University of Hong Kong, 2/F North Wing, Patrick Manson Building, 7 Sassoon Road, Pok Fu Lam, Hong Kong. Tel: + 852 3917 6709; Email: joewu@hku.hk

**Summary**

Prolonged school closure has been adopted worldwide to control COVID-19. Such preemptive implementation was predicated on the premise that school children are a core group for COVID-19 transmission. Using surveillance data from the Chinese cities of Shenzhen and Anqing, we inferred that children aged 18 or below are only around half as susceptible to COVID-19 infection as adults. Using transmission models parameterized with synthetic contact matrices for 152 jurisdictions around the world, we showed that the lower susceptibility of school children substantially limited the effectiveness of school closure in reducing COVID-19 transmissibility. Our results, together with recent findings that clinical severity of COVID-19 in children is lower, suggest that school closure may not be ideal as a sustained, primary intervention for controlling COVID-19.

As the COVID-19 pandemic began to hit different locations during the ongoing first wave, many jurisdictions around the world had preemptively implemented school closure to suppress and mitigate its local spread [1,2]. The UN Educational, Scientific and Cultural Organization (UNESCO) estimated that during April, May and June 2020, around 1.6, 1.2 and 1.1 billion (90%, 68% and 62% )of enrolled learners around the world were affected by country-wide or localized school closure (https://en.unesco.org/covid19/educationresponse). Such swift and widespread adoption of prolonged school closure was largely predicated on the premise that school children would be a core group for COVID-19 transmission as they are for influenza [2]. As countries are now reviewing strategies for social and economic resumption, there is an urgent need to evaluate the rationale and effectiveness of school closure against COVID-19 [3].

Reducing contacts made at school has been effective in controlling influenza because (i) children are biologically more or equally as susceptible to infection compared to adults; (ii) children have more contacts with other children at school than adults have with their peers; and (iii) children are less vigilant about personal infection control (e.g. hand hygiene) compared to adults [4,5]. Indeed, previous epidemiologic studies in different populations have shown that the reproductive number of seasonal influenza and A/H1N1 pandemic influenza in 2009 (H1N1pdm09) was significantly reduced during school closure or holidays (Table 1). While (ii) and (iii) are generally true, it is not clear whether (i) is valid for COVID-19. Although an early analysis of contact tracing and surveillance data from Shenzhen suggested that age has no effect on susceptibility to COVID-19 infection [6], more recent studies indicated that children might only be 35-50% as susceptible as adults [7-9].

On the other hand, there are considerable downsides to prolonged school closure, especially when recent seroprevalence studies suggest that there is yet sufficient population immunity to avert subsequent waves of infection [10,11], likely until a safe and effective vaccine becomes widely available to the majority of the global population that could be a year or longer away. Governments have a duty of care to school-aged children, both for the infection risk of

congregating in schools and at once for their developmental and learning needs if schools are indefinitely suspended. School-aged children with special needs are particularly adversely affected. Of course, parental duties for childcare have been non-trivial and are a cause of widening inequity by socioeconomic position.

We aim to assess the potential impact of school closure in reducing the spread of COVID-19 in different parts of the world. To this end, we first inferred the effect of age on COVID-19 susceptibility and infectiousness using detailed surveillance and contact tracing data from Shenzhen and Anqing, China (the raw data from Shenzhen was the same as that in [6]). We then parameterized our previous age-structured transmission model [12] with the inferred epidemiologic parameters to simulate the epidemiologic impact of school closure in 152 jurisdictions around the world for which contact matrices have been synthesized [13]. To gauge the relative effectiveness of school closure in comparison with other non-pharmaceutical interventions (NPIs), we estimated the reduction in infectious contacts made in non-school settings that would be needed in order to achieve the reduction in transmissibility or schoolchildren infection attack rate (IAR) conferred by school closure.

## Results

### *Household transmission dynamics*

We analyzed within-household transmission of COVID-19 in Shenzhen and Anqing based on the COVID-19 line-lists and outbreak investigation records collated and compiled by the Shenzhen and Anhui Centers for Disease Control and Prevention. Details about these databases have been previously reported (Figure 1A-B) [6,14]. We developed a transmission model to simulate the spread of COVID-19 within households (See Methods for details) and estimated that children were less susceptible to COVID-19 infection than adults (Figure 1C). Specifically, individuals aged 0-12 (primary school age and below) and 13-23 (secondary school and higher education age) were 0.43 (0.21-0.86) and 0.51 (0.27-0.95) times as susceptible to infection as those aged 30 or above, respectively. Although we did not find a significant effect of age on infectiousness

(Figure 1D), the uncertainty in our estimates was large because only 15 primary cases were younger than 20 and they were co-primary cases with their parents or caregivers (Figure 1B). The mean generation time and serial interval was 5.7 (5.1-7.7) days and 5.7% of serial intervals were negative (Figure 1E). Infectiousness peaked when infected individuals were 61% (41-70%) through their incubation period. Consequently, 58% (47-66%) of infections occurred before the infectors developed symptoms. Compared to females, males were equally susceptible to infection but 2.1 (0.8-2.9) times more infectious (Figure 1F). Within-household transmissibility was similar between Shenzhen and Anqing and dropped by 60% (22%-79%) after lockdown measures were implemented in Wuhan on Jan 23 followed by all major Chinese cities shortly after (Figure 1F).

***School closure model***

We extended our previous age-structured model [12] to simulate the impact of school closure on transmission dynamics of COVID-19 and influenza for 152 jurisdictions worldwide for which contact matrices have been synthesized [13]. For COVID-19, we parameterized the model with the maximum likelihood estimates of age-specific susceptibility and infectiousness from our within-household transmission inference. For pandemic influenza, we used the H1N1pdm09 parameters from our previous study which indicated those aged 0-12, 13-18 and 19-29 were 3.8, 2.2 and 1.7 times as susceptible compared to those aged 30 or above [15]. We also considered seasonal influenza for which age had no clear effect on susceptibility or infectiousness.

To avoid underestimating the impact of school closure, we assumed that all contacts made at school would be eliminated during school closure and holidays while contacts in all other settings were unchanged. We estimated the reduction in basic reproductive number ($R_0$) conferred by school closure in each jurisdiction; the reduction in effective reproductive number ($R_t$) would be similar if the age distribution of the susceptible was similar to the overall age distribution (e.g. when most of the population were still susceptible). We estimated the peak prevalence and IAR in each jurisdiction with and without school closure for different values of

$R_0$ (which reflected the baseline transmission dynamics when school closure started, i.e. the combined effect of the intrinsic transmissibility of the virus and the control measures in the population).

***Effectiveness of school closure***

The relative reduction in $R_0$ conferred by school closure was primarily driven by the proportion of contacts made in school (Figure 2A). Our results were consistent with previous studies that had empirically inferred the reduction of the reproductive number for influenza during school closure and holidays in mainland China, France, Hong Kong SAR, India, South Korea and the UK (Table 1).

Because schoolchildren were more than twice as susceptible to H1N1pdm09 compared to adults, school closure could generally reduce the $R_0$ of H1N1pdm09 by 20-50% (except for Qatar and UAE where school contacts accounted for fewer than 10% of all contacts; Figure 2A). In contrast, school closure was much less effective at reducing the $R_0$ of COVID-19, to which children were less susceptible compared to adults (Figure 1C). Specifically, school closure could only reduce the $R_0$ of COVID-19 by 3-10% in high-income populations and populations where school contacts comprised fewer than 20% of all contacts (Figure 2A). This implies that school closure alone would be unable to control COVID-19 in these populations unless the reproductive number was already below 1.03-1.1 (Figure 2B). For lower-middle- and low-income populations, reduction in $R_0$ ranged from 5% (e.g. Vietnam) to 24% (e.g. Uzbekistan); such heterogeneity was again primarily driven by the proportion of contacts made in school. If only kindergartens and primary schools were closed, $R_0$ of COVID-19 in high-, upper-middle-income and other populations would be reduced by 2-5%, 2-12% and 3-20%, respectively. Closing secondary schools and higher education institutions would have similar effects except in low-income populations because they tend to have high out-of-school rates among adolescents and youth of upper secondary school age or above. Similar reductions in $R_0$ conferred by school closure could be achieved by reducing infectious contacts in workplace and community by 4-

16% for high-income populations and 20-50% for populations where school contacts comprised more than 20% of all contacts (Figure 2C). This might be achieved by reducing the frequency or transmissibility (e.g. face mask wearing and heightened personal hygiene) of these contacts. In contrast, this substitution strategy would be too disruptive to be practical or simply impossible for H1N1pdm09 (i.e. the effect of school closure could not be substituted even if all workplace and community contacts were to be eliminated).

For COVID-19, the reduction in morbidity and mortality conferred by school closure would depend on the baseline $R_0$ as well as the timing and duration of school closure (Figure 3). If the baseline $R_0$ was around 2.5 (e.g. the epidemic was largely unmitigated), implementing school closure throughout the epidemic would reduce peak prevalence in high-income and other populations by 6-23% and 12-40%, respectively (Figure 3A). The reductions would be slightly higher for school children (because they are the target group of school closure) and lower for older adults (because physical interactions among children and the elderly are relatively weak in general). In contrast, if the baseline $R_0$ was around 1.5 (e.g. school closure was implemented as a complementary measure in addition to other NPIs), implementing school closure throughout the epidemic would reduce peak prevalence by 14-47% and 23-88% in high-income and other populations, respectively. The reduction in final IAR would be lower than that for peak prevalence. For example, the overall IAR would be reduced by 7-27% and 13-60% in high-income and other populations if $R_0 = 1.5$; the corresponding reductions were 3-10% and 6-14% if $R_0 = 2.5$. Reducing infectious contacts in non-school settings by 8-21% and 13-35% in high-income and other populations, respectively, would achieve the reduction in IAR under 18 conferred by school closure if $R_0 = 1.5$; the corresponding reduction requirement would increase to 18-40% for all populations if $R_0 = 2.5$.

Note that these comparative outcomes across jurisdictions are conditional on the baseline $R_0$ which is not necessarily the same in all populations due to heterogeneity in age structures, contact patterns, climactic factors and intervention policies. Importantly thus, our results do not

suggest that prevalence and IAR would generally be lower in high-income populations or that school closure would generally confer greater reductions in peak prevalence and IAR in lower-middle-income and low-income populations.

**Discussion**

The fundamental motivation for school closure presumes schoolchildren are a core transmission group. In concordance with recent studies [7-9], we have shown that this premise turns out to be invalid because compared to older individuals, school children are substantially less susceptible to COVID-19. Consequently, even prolonged school closure would have limited effectiveness in reducing transmissibility, especially in high-income and upper-middle-income populations where school contacts generally comprise fewer than 20% of all contacts.

Our results, together with recent findings that clinical severity of COVID-19 in children is lower than that for adults [12,16] and that prolonged school closure could significantly impair the emotional, mental and physical health of schoolchildren (see below), suggest that school closure may not be ideal as a sustained primary NPI for controlling COVID-19. In fact, the specific objective underlying school closure should be more clearly articulated so that alternative options could be comparatively assessed. For example, if the objective is to minimize IAR among school-aged children, the same outcome could be attained by reducing infectious contacts in non-school settings (e.g. by enhancing personal infection prevention) which is likely to be more feasible and less detrimental to children's overall wellbeing. On the other hand, short-term school suspension could and should be considered when other NPIs (e.g. avoidance of mass gatherings, physical distancing in workplace and community, enhanced personal hygiene, etc.) are already in place, where the marginal effect of school closure is critical to achieving the target control levels (e.g. when hospitals have exceeded their surge capacity and clinical outcomes including the case-fatality risk are on the verge of unnecessarily deteriorating simply because the health system is about to implode).

Recent studies have highlighted numerous downsides of prolonged school closure on the mental and physical well-being of children, including increased risks of loneliness, academic achievement gaps, reduction in physical activity, malnutrition (for children who rely on school meals), increased risk of domestic abuse and violence, etc. [17-21]. Even within high-income populations, these adverse effects would likely be disproportionately amplified among socio-economically disadvantaged groups (e.g. lack of or limited access to childcare, technical and financial support for digital learning, online social interactions and physical exercises). In addition, closing schools could inadvertently cause childcare shortages and hence worker absenteeism among parents. The resulting worker absenteeism in the healthcare system (which has been estimated to be around 20% for the US health-care workforce) could indirectly exacerbate the case-fatality risk of COVID-19 patients and therefore the overall mortality rate of the pandemic due to weakened healthcare [22]. As such, compensatory measures should be proactively devised to ameliorate these adverse events if school closure is employed to control COVID-19. For example, child-care arrangement should be explicitly considered in order to minimize unintended worker absenteeism and the downstream adverse effect on healthcare quality.

We estimated that within-household transmissibility in Shenzhen and Anqing was reduced by 60% (22%-79%) in Jan-Mar after nationwide lockdown measures were implemented in China. Given that human mobility in all Chinese major cities was reduced by >90% during this period, such reduction in within-household transmissibility was likely due to heightened precautions of personal infection prevention. Sustained adoption of such precautions in the 152 jurisdictions could in principle reduce the reproductive number of COVID-19 by 5-21% which would be comparable to that conferred by school closure.

Our study has several limitations. First, we assumed that school closure would eliminate all school contacts without affecting contacts in either settings. In reality, school closure would increase some non-school contacts (e.g. more contacts between children and their caregivers),

in which case school closure would be less effective than estimated here. Second, we assumed that age had no effect on infectiousness [23]. If children are less infectiousness than adults, as postulated by recent studies [24], then school closure would be less effective than estimated here. Third, our framework is built on the contact matrices synthesized by Prem et al. [13] which have been increasingly used to study infectious diseases including COVID-19 [7,25,26]. Although our results are consistent with published estimates in the context of H1N1pdm09 and seasonal influenza (Table 1), thus giving credence to epidemiologic validity of our framework, the general validity of synthetic contact matrices would require more extensive validation against empirical social contact surveys and seroepidemiological studies. This highlights the critical importance of conducting periodic social contact surveys in different parts of the world for informing epidemic surveillance and control of a wide range of infectious diseases including COVID-19, influenza, TB, RSV, measles, etc. Finally, we must remain alert to the evolving understanding about the multisystem inflammatory syndrome in children associated with COVID-19 [27], especially as it relates to whether ethnic or other special subgroups amongst this age cohort could be particularly susceptible to this phenotype [28].

## Methods

### *Data on within-household transmission*

We analyzed within-household transmission of COVID-19 in Shenzhen and Anqing based on the COVID-19 line-lists and outbreak investigation records collated and compiled by the Shenzhen and Anhui Centers for Disease Control and Prevention. Details about these databases have been previously reported [6,14]. For this study, we first identified cases who were almost certainly infected outside their household based on their travel and contact history. We then inferred the membership of their households based on outbreak investigation records. After excluding households with more than 8 members (because they were rare and we were relatively uncertain whether these clusters were *bona fide* households), our dataset comprised a total of 182 household clusters (147 from Shenzhen and 35 from Anhui; see Figures S1-S13) with 238 primary/co-primary cases and 599 household contacts.

### *Household transmission model*

We developed a transmission model to simulate the spread of COVID-19 within households assuming that within each household, all non-primary cases were secondary cases generated by the primary/co-primary cases (i.e. no tertiary cases). We assumed that among household contacts, the risk of community transmission was negligible compared to the force of infection exerted by the primary/co-primary cases. We inferred the following parameters by fitting the model to the data: (i) age-specific susceptibility to infection; (ii) age-specific infectiousness; (iii) relative susceptibility and infectiousness of males compared to females; (iv) baseline transmissibility for each household size; (iv) the generation time distribution; (v) the transmissibility in Anqing relative to Shenzhen; and (vi) changes in within-household transmissibility after nationwide lockdown measures were implemented.

We use $\theta$ to denote the set of parameters subject to statistical inference.

*Infectiousness profile and generation time distribution*. Suppose individual *j* was infected by individual *i*. We used $f_{inc}(\cdot)$ to denote the probability density function (pdf) of the incubation period and assumed that their incubation periods are independent and denoted them by $X_i$ and $X_j$, respectively. Let $Y$ be the time it took for individual *i* to infect individual *j* after the former had become infected (i.e. the generation time for this pair). We assumed that the of $Y$ was dependent on $X_i$ as follows:

$$P(Y = y|X_i = x) = f_{gen}(y|\theta, x) = \begin{cases} 0 & \text{if } y < \mu_{inf}x; \\ g(y - \mu_{inf}x|a_{inf}, b_{inf}) & \text{if } y \geq \mu_{inf}x. \end{cases}$$

where $g(\cdot\,|a, b)$ was the gamma pdf with shape $a$ and scale $b$, $\mu_{inf}x$ was the time at which individual *i* became infectious which was assumed to increase linearly with the incubation time $x$. We assumed that the time it took infectiousness to peak after the infected individual had become infectious was $\rho_{inf}x$ (such that $b_{inf} = \rho_{inf}x/(a_{inf} - 1)$). See Figures S1-S13 for the schematic. The parameters $(\mu_{inf}, a_{inf}, \rho_{inf})$ were included in $\theta$ for statistical inference. The pdf of the generation time for individuals *i* and *j* was

$$f_{gen}(y|\theta) = P(Y = y) = \int_0^\infty P(Y = y\,|X_i = x)f_{inc}(x)dx = \int_0^\infty f_{gen}(y|\theta, x)f_{inc}(x)dx$$

The pdf of the serial interval for individuals *i* and *j*, namely $Z = Y + X_j - X_i$, was

$$f_{SI}(y|\theta) = P(Z = z) = P\big(Y + X_j - X_i = z\big) = \int_0^\infty P\big(Y + X_j = z + x\,\big|X_i = x\big)f_{inc}(x)dx$$

where

$$P\big(Y + X_j = z + x\,\big|X_i = x\big) = \int_0^{z+x} P\big(X_j = z + x - u\,\big|X_i = x\big)f_{gen}(u)du = \int_0^{z+x} f_{inc}(z + x - u)f_{gen}(u|\theta, x)du$$

We assumed that the incubation period distribution was lognormal with median 5.1 days and mean 5.5 days [29].

*Statistical inference of transmission parameters.* The overall likelihood function was

$$L(\theta) = \prod_k L_k(\theta)\, L_{SI}(\theta) \prod_{j \in A} f_{SI}(s_j|\theta) \prod_{j \in B} F_{SI}(s_j^U|\theta) - F_{SI}(s_j^L|\theta)$$

where $L_k(\theta)$ was the likelihood function for the cluster k and $L_{SI}(\theta)$ was the likelihood for serial interval data collected from outside Anqing and Shenzhen. These likelihood functions were formulated as follows.

We partitioned each cluster $k$ into three sets of individuals:

- Set $A_k$ comprised all the primary cases (i.e. those who were infected outside and introduced the infection into the cluster).
- Set $B_k$ comprised all members who were infected during the cluster outbreak initiated by the primary cases in $A_k$.
- Set $C_k$ comprised all members who were not infected during the cluster outbreak initiated by the primary cases in $A_k$.

In our dataset, very few clusters had more than one contact infected (Figures S1-S13). As such, for model simplicity, we assumed that all infected contacts were infected by the primary cases (i.e. no tertiary infections). Let $a_i$ and $g_i$ be the age and sex of individual $i$, and $T_i$ and $O_i$ be the time of infection and time of symptoms onset if he/she was infected (i.e. $i \in A_k$ or $i \in B_k$), respectively. Our aim was to infer the following epidemiologic characteristics of COVID-19:

1. The effect of age on susceptibility to infection.
2. The effect of age on infectiousness.
3. The effect of sex on susceptibility to infection.
4. The effect of sex on infectiousness.
5. Transmission rate for cluster with sizes $n = 2, ..., 8$.

6. The relative within-household transmissibility of COVID-19 in clusters from Anqing compared to that from Shenzhen.
7. The relative within-household transmissibility of COVID-19 after lockdown measures were implemented in Wuhan on Jan 23 followed by all major Chinese cities shortly after.
8. The pdf of the generation time ($f_{gen}$; see previous subsection).

Based on the travel and contact history of the infected cases, outbreak investigators were able to specify a range for their time of infection. We denoted this range by $[T_{min,i}, T_{max,i}]$ for individual $i \in A_k$ or $i \in B_k$, i.e. $T_{min,i} \leq T_i \leq T_{max,i}$. The likelihood for cluster *k* conditioned on the time of infection of its primary cases (i.e. $T_i, i \in A_k$) was formulated as follows:

$$L_k(\theta|T_i, i \in A_k) = \prod_{m=1}^{3} L_{k,m}(\theta|T_i, i \in A_k)$$

where

1. $L_{k,1}(\theta|T_i, i \in A_k) = \prod_{i \in A_k} f_{inc}(O_i - T_i)$ was the probability that individual $i \in A_k$ (i.e. the index cases) developed symptoms at time $O_i$ given that he/she was infected at time $T_i$.
2. $L_{k,2}(\theta|T_i, i \in A_k) = \prod_{i \in B_k} \int_{T_{min,i}}^{T_{max,i}} \Lambda_i(T_i) \exp\left(-\int_0^{T_i} \Lambda_i(t)dt\right) f_{inc}(O_i - T_i)dT_i$ was the probability that each individual $i \in B_k$ (i.e. all contacts that became infected during the cluster outbreak) was infected between time $T_{min,i}$ and $T_{max,i}$ and developed symptoms at time $O_i$. The force of infection on individual *i* was $\Lambda_i(t) = \sum_{j \in A_k} \lambda_{ji}(t)$ where $\lambda_{ji}(t)$ was the force of infection exerted by individual *j* on individual *i* at time *t.* We modelled the latter using the equation

$$\lambda_{ji}(t) = \omega(k)L(t)\beta(n_i)\delta_{inf}(g_j)\delta_{sus}(g_i)\alpha(a_i)f_{gen}(t - T_j|\theta, O_j - T_j)Q_{ij}(t)$$

where:

- $\omega(k)$ was the relative transmission rate for clusters in Anqing compared to those in Shenzhen, i.e. $\omega(k) = \omega_{AQ}$ if cluster $k$ was from Anqing and 1 if it was from Shenzhen.
- $L(t)$ was the relative transmission rate after Wuhan was locked down, i.e. $L(t) = \sigma$ if time $t$ was after 23 January 2020 and 1 otherwise.
- $\beta(n)$ was the baseline transmission rate for clusters with $n$ members.
- $\delta_{inf}(\cdot)$ was sex-specific infectiousness (assumed to be 1 for females).
- $\delta_{sus}(\cdot)$ was sex-specific susceptibility (assumed to be 1 for females).
- $\alpha_{inf}(\cdot)$ was age-specific infectiousness which was assumed to be: (i) equal to 1 for those aged 40 years or above; and (ii) a piece-wise cubic Hermite interpolating polynomial function (https://www.mathworks.com/help/matlab/ref/pchip.html) of age for those aged under 40 years where the value of $\alpha_{inf}(0)$ was included in $\theta$ for statistical inference.
- $\alpha_{sus}(\cdot)$ was age-specific susceptibility which was assumed to be: (i) equal to 1 for those aged 30 years or above; and (ii) a piece-wise cubic Hermite interpolating polynomial function (https://www.mathworks.com/help/matlab/ref/pchip.html) of age for those aged under 30 years where the value of $\alpha_{sus}(\cdot)$ at age 0 and 15 years were included in $\theta$ for statistical inference.
- $Q_{ij}(t) = 1$ if individual $j$ was exposed to individual $i$ at time $t$ and 0 otherwise (see Figure S1).

3. $L_{k,3}(\theta|T_i, i \in A_k) = \prod_{i \in C_k} \exp\left(-\int_0^{T_k^*} \Lambda_i(u)du\right)$ was the probability that individual $i \in C_k$ (i.e. all uninfected contacts) remained uninfected by the end of the cluster outbreak (time $T_k^*$).

The overall likelihood for cluster $k$ was

$$L_k(\theta) = \int_{\Omega_k} L_k(\theta|T_i, i \in A_k) \prod_{i \in A_k} h_{inf,i}(T_i) dT_i$$

where $\Omega_k$ was the Cartesian product of $[T_{min,i}, T_{max,i}]$ for all $i \in A_k$ and $h_{inf,i}$ was the pdf of the time of infection for individual $i \in A_k$. Let $T_{lockdown}$ denote the time when Wuhan was locked down (i.e. 23 January 2020). Given that (1) primary cases had history of travelling to or were residents of Hubei, or had contact history with suspected cases or returnees from Hubei; and (2) community transmission of COVID-19 in Shenzhen and Anqing was relatively low during the study time horizon, we assumed that the probability of $T_i = t$ was proportional to the epidemic size in Wuhan at time $t$ if time $t < T_{lockdown}$ and zero otherwise. That is,

$h_{inf,i}(T_i) = e^{rT_i} \Big/ \int_{T_{min,i}}^{T^*_{max,i}} e^{r\tau}\, d\tau = re^{rT_i} / (e^{rT^*_{max,i}} - e^{rT_{min,i}})$ for $T_{min,i} \le t \le T^*_{max,i}$ where $r$ was the epidemic growth rate in Wuhan (assumed to be 0.133 day$^{-1}$ which corresponded to a doubling time of 5.2 days[12]) and $T^*_{max,i} = \min(T_{max,i}, T_{lockdown})$. In this likelihood formulation, we have assumed that given one or more primary case in any given cluster, the force of infection from community transmission on the cluster members was negligible.

We estimated the model parameters $\theta$ using Markov Chain Monte Carlo methods with Gibbs sampling and non-informative flat prior. Point estimates and statistical uncertainty were presented using the maximum posteriori probability (MAP) estimate and 95% credible intervals (CrIs), respectively. Because flat prior was used, the MAP estimate was the same as the maximum likelihood estimate.

***Age-structured transmission model***

We partitioned the population of each jurisdiction into the following $m$ = 15 age groups: 0-3, 4-12, 13-18, 19-23, 24-29, 30-34, 35-39, 40-44, 45-49, 50-54, 55-59, 60-64, 65-69, 70-74 and 75+. We assumed that age had no effect on infectiousness. Let $\alpha_i$ be the relative susceptibility of age group $i$. For COVID-19, we parameterized $\alpha_i$'s according to Figure 1C. For H1N1pdm09, we

parameterized $\alpha_i$'s according to our previous study which indicated those aged 0-12, 13-18 and 19-29 were 3.8, 2.2 and 1.7 times as susceptible compared to those aged 30 or above [15].

We used the following SIR model to simulate COVID-19 and influenza epidemics where $S_i(t)$, and $R_i(t)$ were the number of susceptible and recovered individuals in age group *i* at time *t*, and $I(t,\tau)$ was the number of infected individuals in age group *i* at time *t* who were infected at time $t-\tau$:

$$\frac{dS_i(t)}{dt} = -\alpha_i S_i(t)\pi_i(t)$$

$$\frac{\partial I_i(t,\tau)}{\partial t} + \frac{\partial I_i(t,\tau)}{\partial \tau} = -f_{gen}(\tau) I_i(t,\tau)$$

$$I_i(t,0) = \alpha_i S_i(t)\pi_i(t)$$

$$\frac{dR_i(t)}{dt} = \int_0^t f_{gen}(\tau) I_i(t,\tau) d\tau$$

$$\pi_i(t) = \sum_{j=1}^{m} \frac{\beta_{ij}}{N_j} \int_0^t I_j(t,\tau) d\tau,$$

where $\{\beta_{ij}\}11$ was the contact matrix obtained from Prem et al [13] and $N_1, \ldots, N_1$ was the age distribution obtained from World Population Prospects 2019 (https://population.un.org/wpp/DataQuery/). The next generation matrix (NGM) for this SIR model was

$$\frac{T_G}{N}\begin{bmatrix} \alpha_1\beta_{11}N_1 & \cdots & \alpha_1\beta_{1m}N_1 \\ \vdots & \ddots & \vdots \\ \alpha_m\beta_{m1}N_m & \cdots & \alpha_m\beta_{mm}N_m \end{bmatrix}$$

where $T_G$ was the mean generation time. The basic reproductive number $R_0$ was the largest eigenvalue of this matrix.

The synthetic contact matrices from Prem et al [13] could be decomposed by the settings in which contacts were made: household, school, workplace and community. In our model, if school

closure was implemented, all contacts made at school were removed from the contact matrix and the resulting NGM was used to calculate the reproductive number. Similarly, when the frequency or transmissibility of contacts made in a given setting (e.g. community) was reduced by $x$%, the contact matrix of that setting was discounted by $x$% accordingly.

**Funding**

This research was supported by a commissioned grant from the Health and Medical Research Fund from the Government of the Hong Kong Special Administrative Region, The Fundamental Research Funds for the Central Universities (Grant number. YD9110004001, YD9110002002, and YD9110002008), Shenzhen Key Medical Discipline Construction Fund (SZXK064) and National Natural Science Foundation of China (General Program, No.41771441). The funding body had no role in study design, data collection and analysis, preparation of the manuscript, or the decision to publish.

**Contributors**

J. T. W., K. L., and G. M. L. designed the experiments. S. M., S. L., Q. L., J. L. Y. L., J. W., T. F., X. Z. collected data. J. T. W., K. L., and D. L. analyzed data. J. T. W., K. L., and G. M. L. interpreted the results. J. T. W., and G. M. L. wrote the manuscript. All authors have seen and approved the manuscript. All authors have contributed significantly to the work.

**Declaration of interests**

The authors declare no competing interests.

**Data sharing statement**

All data are available in the main text or the supplementary materials.

**References**


1 Wang, G., Zhang, Y., Zhao, J., Zhang, J. & Jiang, F. Mitigate the effects of home confinement on children during the COVID-19 outbreak. *The Lancet* **395**, 945-947 (2020).

2 Viner, R. M. *et al.* School closure and management practices during coronavirus outbreaks including COVID-19: a rapid systematic review. *Lancet Child Adolesc Health* **4**, 397-404, doi:10.1016/S2352-4642(20)30095-X (2020).

3 Esposito, S. & Principi, N. School Closure During the Coronavirus Disease 2019 (COVID-19) Pandemic: An Effective Intervention at the Global Level? *JAMA Pediatr*, doi:10.1001/jamapediatrics.2020.1892 (2020).

4 Fong, M. W. *et al.* Nonpharmaceutical measures for pandemic influenza in nonhealthcare settings—social distancing measures. *Emerging infectious diseases* **26**, 976 (2020).

5 Xiao, J. *et al.* Nonpharmaceutical measures for pandemic influenza in nonhealthcare settings—personal protective and environmental measures. *Emerging infectious diseases* **26**, 967 (2020).

6 Bi, Q. *et al.* Epidemiology and transmission of COVID-19 in 391 cases and 1286 of their close contacts in Shenzhen, China: a retrospective cohort study. *Lancet Infect Dis*, doi:10.1016/S1473-3099(20)30287-5 (2020).

7 Davies, N. G. *et al.* Age-dependent effects in the transmission and control of COVID-19 epidemics. *Nat Med*, doi:10.1038/s41591-020-0962-9 (2020).

8 Jing, Q. L. *et al.* Household secondary attack rate of COVID-19 and associated determinants in Guangzhou, China: a retrospective cohort study. *Lancet Infect Dis*, doi:10.1016/S1473-3099(20)30471-0 (2020).

9 Zhang, J. *et al.* Changes in contact patterns shape the dynamics of the COVID-19 outbreak in China. *Science* **368**, 1481-1486, doi:10.1126/science.abb8001 (2020).

10 Pollán, M. *et al.* Prevalence of SARS-CoV-2 in Spain (ENE-COVID): a nationwide, population-based seroepidemiological study. *The Lancet*, doi:10.1016/S0140-6736(20)31483-5.

11 Stringhini, S. *et al.* Seroprevalence of anti-SARS-CoV-2 IgG antibodies in Geneva, Switzerland (SEROCoV-POP): a population-based study. *The Lancet*, doi:10.1016/S0140-6736(20)31304-0.

12 Wu, J. T. *et al.* Estimating clinical severity of COVID-19 from the transmission dynamics in Wuhan, China. *Nature Medicine*, doi:10.1038/s41591-020-0822-7 (2020).

13 Prem, K., Cook, A. R. & Jit, M. Projecting social contact matrices in 152 countries using contact surveys and demographic data. *PLoS Comput Biol* **13**, e1005697, doi:10.1371/journal.pcbi.1005697 (2017).

14 Zheng, X. *et al.* Asymptomatic patients and asymptomatic phases of Coronavirus Disease 2019 (COVID-19): a population-based surveillance study. *National Science Review* (2020).

15 Wu, J. T. *et al.* Inferring influenza infection attack rate from seroprevalence data. *PLoS Pathog* **10**, e1004054, doi:10.1371/journal.ppat.1004054 (2014).

16 Verity, R. *et al.* Estimates of the severity of coronavirus disease 2019: a model-based analysis. *Lancet Infect Dis* **20**, 669-677, doi:10.1016/S1473-3099(20)30243-7 (2020).

17 Mayurasakorn, K., Pinsawas, B., Mongkolsucharitkul, P., Sranacharoenpong, K. & Damapong, S. N. School closure, COVID-19 and lunch programme: Unprecedented undernutrition crisis in low-middle income countries. *J Paediatr Child Health*, doi:10.1111/jpc.15018 (2020).

18 Thomas, E. Y., Anurudran, A., Robb, K. & Burke, T. F. Spotlight on child abuse and neglect response in the time of COVID-19. *Lancet Public Health* **5**, e371, doi:10.1016/S2468-2667(20)30143-2 (2020).

19 Loades, M. E. *et al.* Rapid Systematic Review: The Impact of Social Isolation and Loneliness on the Mental Health of Children and Adolescents in the Context of COVID-19. *J Am Acad Child Adolesc Psychiatry*, doi:10.1016/j.jaac.2020.05.009 (2020).

20 S, S. S. T. & Griffiths, G. Child protection in the time of COVID-19. *J Paediatr Child Health* **56**, 838-840, doi:10.1111/jpc.14916 (2020).

21 Green, P. Risks to children and young people during covid-19 pandemic. *BMJ* **369**, m1669, doi:10.1136/bmj.m1669 (2020).

22 Bayham, J. & Fenichel, E. P. Impact of school closures for COVID-19 on the US health-care workforce and net mortality: a modelling study. *Lancet Public Health* **5**, e271-e278, doi:10.1016/S2468-2667(20)30082-7 (2020).

23 Jones, T. C. *et al.* An analysis of SARS-CoV-2 viral load by patient age. *medRxiv*, 2020.2006.2008.20125484, doi:10.1101/2020.06.08.20125484 (2020).

24 Bunyavanich, S., Do, A. & Vicencio, A. Nasal Gene Expression of Angiotensin-Converting Enzyme 2 in Children and Adults. *JAMA* **323**, 2427-2429, doi:10.1001/jama.2020.8707 (2020).

25 Koo, J. R. *et al.* Interventions to mitigate early spread of SARS-CoV-2 in Singapore: a modelling study. *The Lancet Infectious Diseases* (2020).

26 Hilton, J. & Keeling, M. J. Estimation of country-level basic reproductive ratios for novel Coronavirus (SARS-CoV-2/COVID-19) using synthetic contact matrices. *PLOS Computational Biology* **16**, e1008031, doi:10.1371/journal.pcbi.1008031 (2020).

27 Feldstein, L. R. *et al.* Multisystem Inflammatory Syndrome in US Children and Adolescents. *New England Journal of Medicine* (2020).

28 Kam, K.-Q., Ong, J. S. & Lee, J. H. Kawasaki disease in the COVID-19 era: a distinct clinical phenotype? *The Lancet Child & Adolescent Health* (2020).

29 Lauer, S. A. *et al.* The Incubation Period of Coronavirus Disease 2019 (COVID-19) From Publicly Reported Confirmed Cases: Estimation and Application. *Ann Intern Med* **172**, 577-582, doi:10.7326/M20-0504 (2020).

30 Birrell, P. J. *et al.* Bayesian modeling to unmask and predict influenza A/H1N1pdm dynamics in London. *Proc Natl Acad Sci U S A* **108**, 18238-18243, doi:10.1073/pnas.1103002108 (2011).

31 Ali, S. T., Kadi, A. S. & Ferguson, N. M. Transmission dynamics of the 2009 influenza A (H1N1) pandemic in India: the impact of holiday-related school closure. *Epidemics* **5**, 157-163, doi:10.1016/j.epidem.2013.08.001 (2013).

32 Yu, H. *et al.* Transmission dynamics, border entry screening, and school holidays during the 2009 influenza A (H1N1) pandemic, China. *Emerg Infect Dis* **18**, 758-766, doi:10.3201/eid1805.110356 (2012).

33 Cauchemez, S., Valleron, A. J., Boelle, P. Y., Flahault, A. & Ferguson, N. M. Estimating the impact of school closure on influenza transmission from Sentinel data. *Nature* **452**, 750-754, doi:10.1038/nature06732 (2008).

34 Ali, S. T., Cowling, B. J., Lau, E. H. Y., Fang, V. J. & Leung, G. M. Mitigation of Influenza B Epidemic with School Closures, Hong Kong, 2018. *Emerg Infect Dis* **24**, 2071-2073, doi:10.3201/eid2411.180612 (2018).

35 Ryu, S., Ali, S. T., Cowling, B. J. & Lau, E. H. Y. Effects of school holidays on seasonal influenza in South Korea, 2014-2016. *J Infect Dis*, doi:10.1093/infdis/jiaa179 (2020).

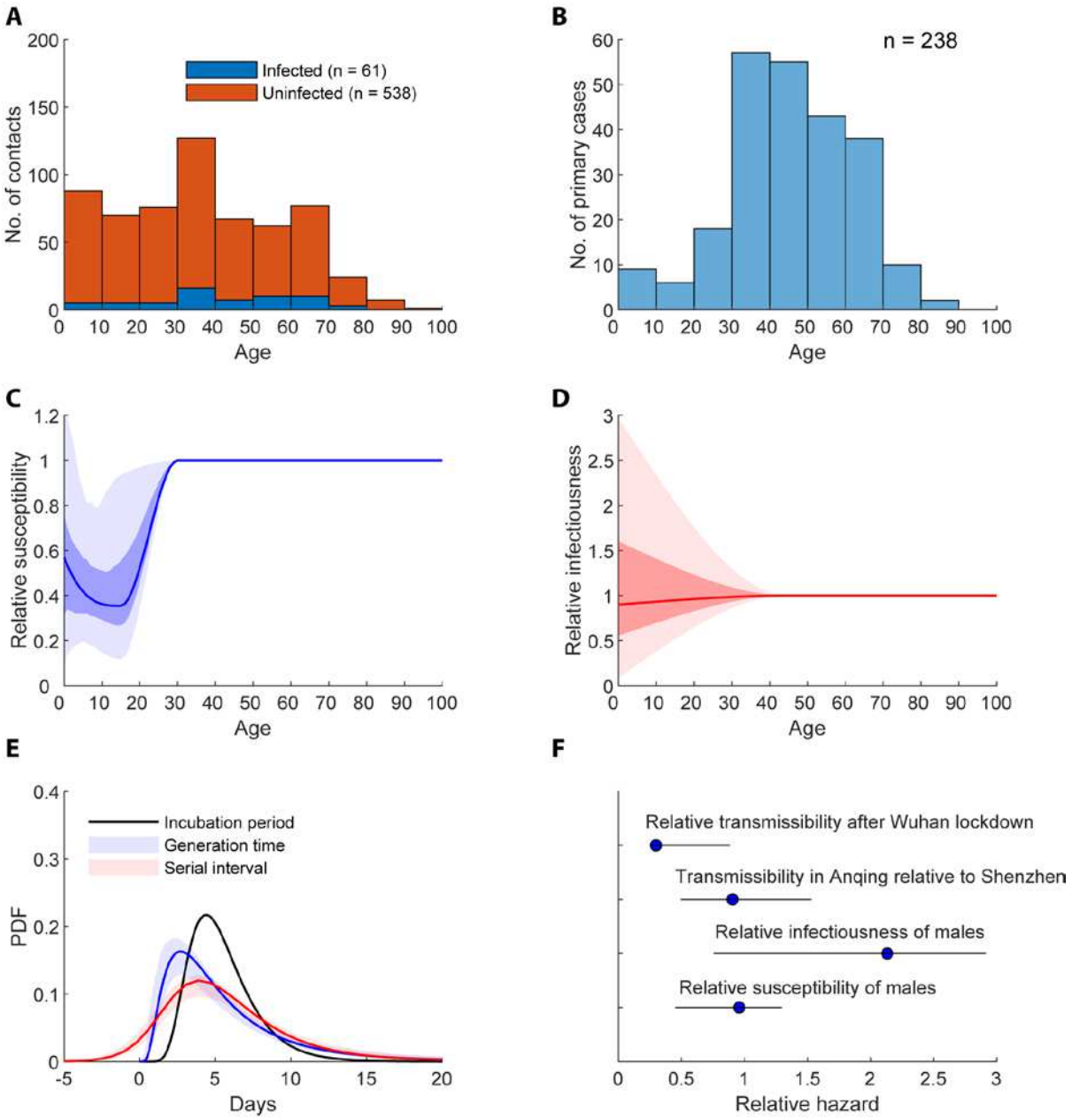


**Figure 1. Within-household transmission dynamics of COVID-19 among 182 clusters in Shenzhen and Anqing.** Key assumptions included: the incubation period distribution was lognormal with median 5.1 days and mean 5.5 days [29]; susceptibility was the same for those aged 30 or above; infectiousness was the same for those aged 40 or above. **A**-**B** Age distribution of household contacts (stratified by infection outcome) and primary cases. **C-F** Age-specific susceptibility, age-specific infectiousness, generation time distribution and serial interval distribution. Lines, dark shades and light shades correspond to MAP estimates, 50% CrIs and 95% Crls, respectively. **F** Susceptibility and infectiousness of males relative to females;

transmissibility in Anqing relative to Shenzhen; and relative transmissibility after vs before Wuhan lockdown. Circles and bars correspond to MAP estimates (equivalent to maximum likelihood estimates because flat prior was used in the inference) and 95% CrIs.

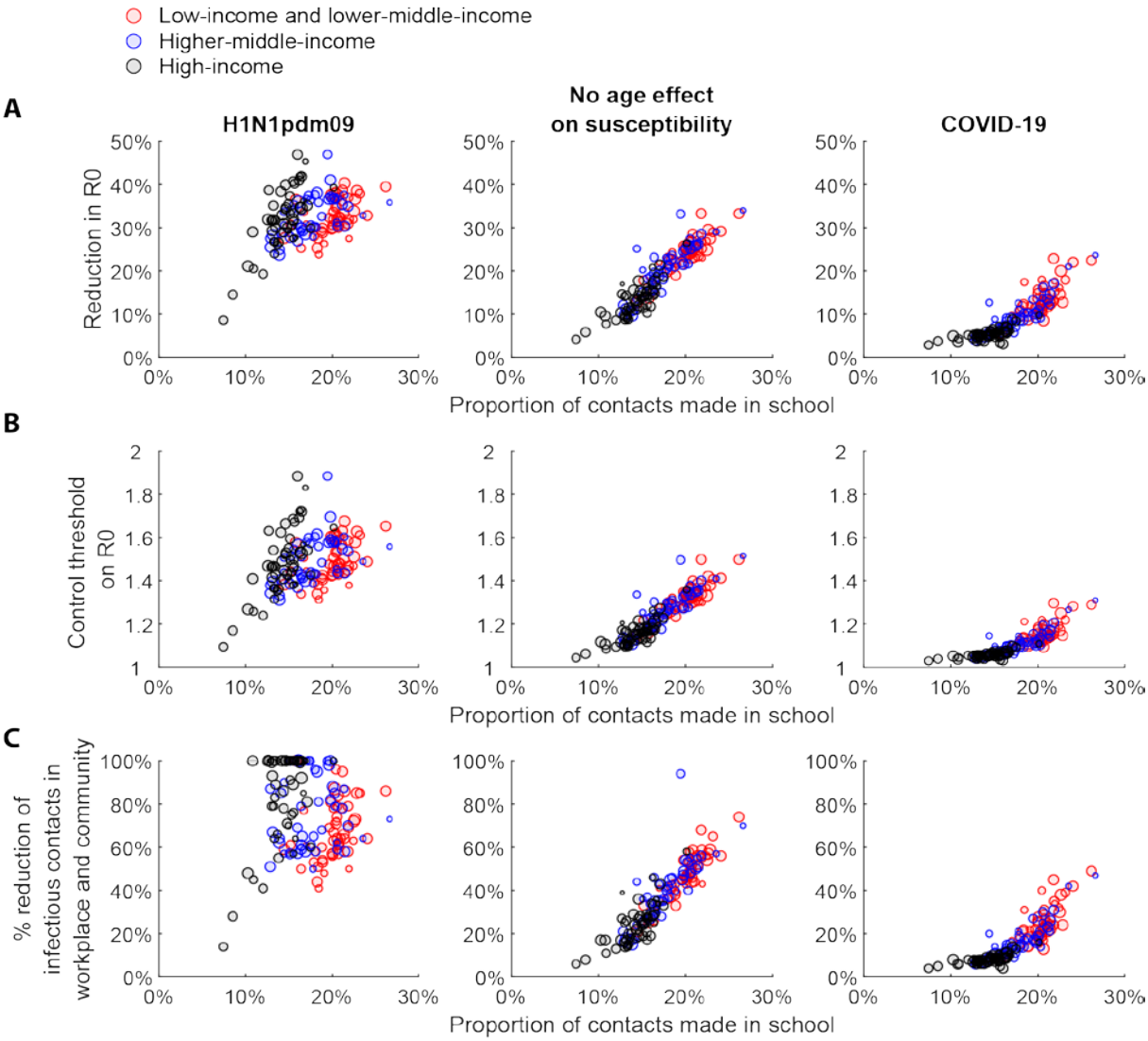


**Figure 2. The effectiveness of school closure in reducing transmissibility as a function of proportion of contacts made in school across 152 jurisdictions.** See Table S1 for the numerical values of all data points shown here. The sizes of data points are proportional to the log of the corresponding population size. **A** Reduction in R0 conferred by school closure against H1N1pdm09 (left), a pathogen to which individual of all ages were equally susceptible (middle) and COVID-19 (right). **B** Outbreak threshold (in terms of R0) under school closure. **C** Percent reduction in workplace and community contacts that would be required in order to achieve the reduction in R0 conferred by school closure. A required percentage of 100% (for some high-income and upper-middle-income populations in the case of H1N1pdm09) means that this was impossible.

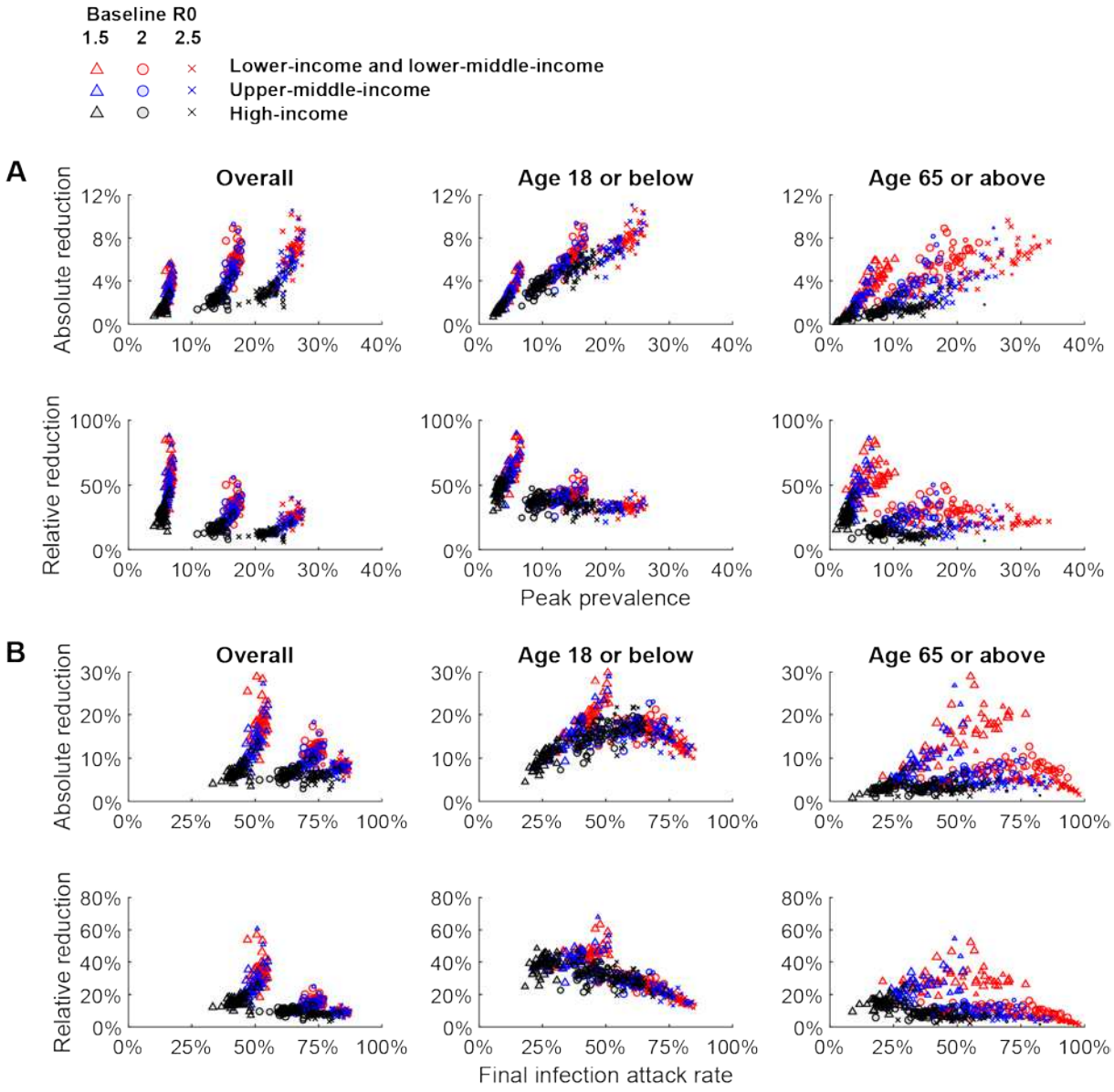


**Figure 3. The public health impact of school closure across 152 jurisdictions.** See Table S1 for the numerical values of all data points shown here. **A** Reduction in peak prevalence for all ages (left), those aged 18 or below (middle) and those aged 65 or above (right). **B** Reduction in final IAR for all ages (left), those aged 18 or below (middle) and those aged 65 or above (right).

**Table 1. Comparison between our results and published estimates of reduction in reproductive number for H1N1pdm09 and seasonal influenza during school closure and holidays.**

| | **Published estimates** | **Our estimates** |
|---|---|---|
| H1N1pdm09 in the UK during summer holidays [30] | 35% (30-40%) | 33% |
| H1N1pdm09 in HK during closure of kindergartens and primary schools [15] | 13% (10-15%) | 17% |
| H1N1pdm09 in HK during summer holidays [15] | 35% | 35% |
| H1N1pdm09 in India during summer holidays [31] | 14-27% | 38% |
| H1N1pdm09 in China during school holidays [32] | 37% (28-45%) | 36% |
| Seasonal influenza in France during summer holidays in 1985-2006 [33] | 13-17% | 12% if no age effect<br>32% if H1N1pdm09-like |
| Seasonal influenza B in Hong Kong during closure of kindergartens and primary schools in 2018 [34] | 16% (10-26%) | 5% if no age effect<br>17% if H1N1pdm09-like |
| Seasonal influenza in South Korea during school holidays in 2014-2016 [35] | 6-23% | 18% if no age effect<br>40% if H1N1pdm09-like |

# Figures

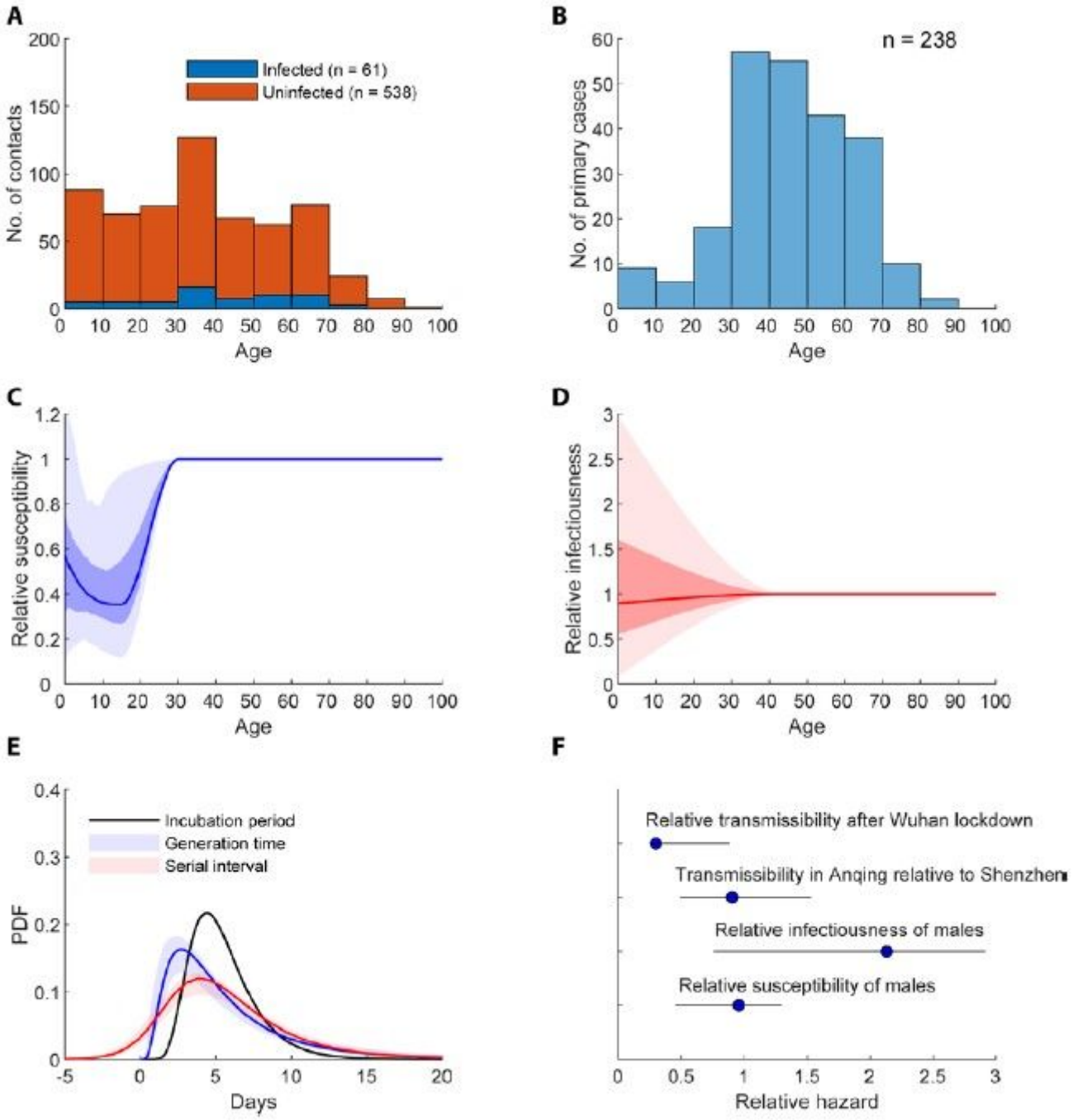


**Figure 1**

Within-household transmission dynamics of COVID-19 among 182 clusters in Shenzhen and Anqing. Key assumptions included: the incubation period distribution was lognormal with median 5.1 days and mean 5.5 days 29; susceptibility was the same for those aged 30 or above; infectiousness was the same for those aged 40 or above. A-B Age distribution of household contacts (stratified by infection outcome) and primary cases. C-F Age-specific susceptibility, age-specific infectiousness, generation time distribution and serial interval distribution. Lines, dark shades and light shades correspond to MAP estimates, 50%

CrIs and 95% CrIs, respectively. F Susceptibility and infectiousness of males relative to females; transmissibility in Anqing relative to Shenzhen; and relative transmissibility after vs before Wuhan lockdown. Circles and bars correspond to MAP estimates (equivalent to maximum likelihood estimates because flat prior was used in the inference) and 95% CrIs.

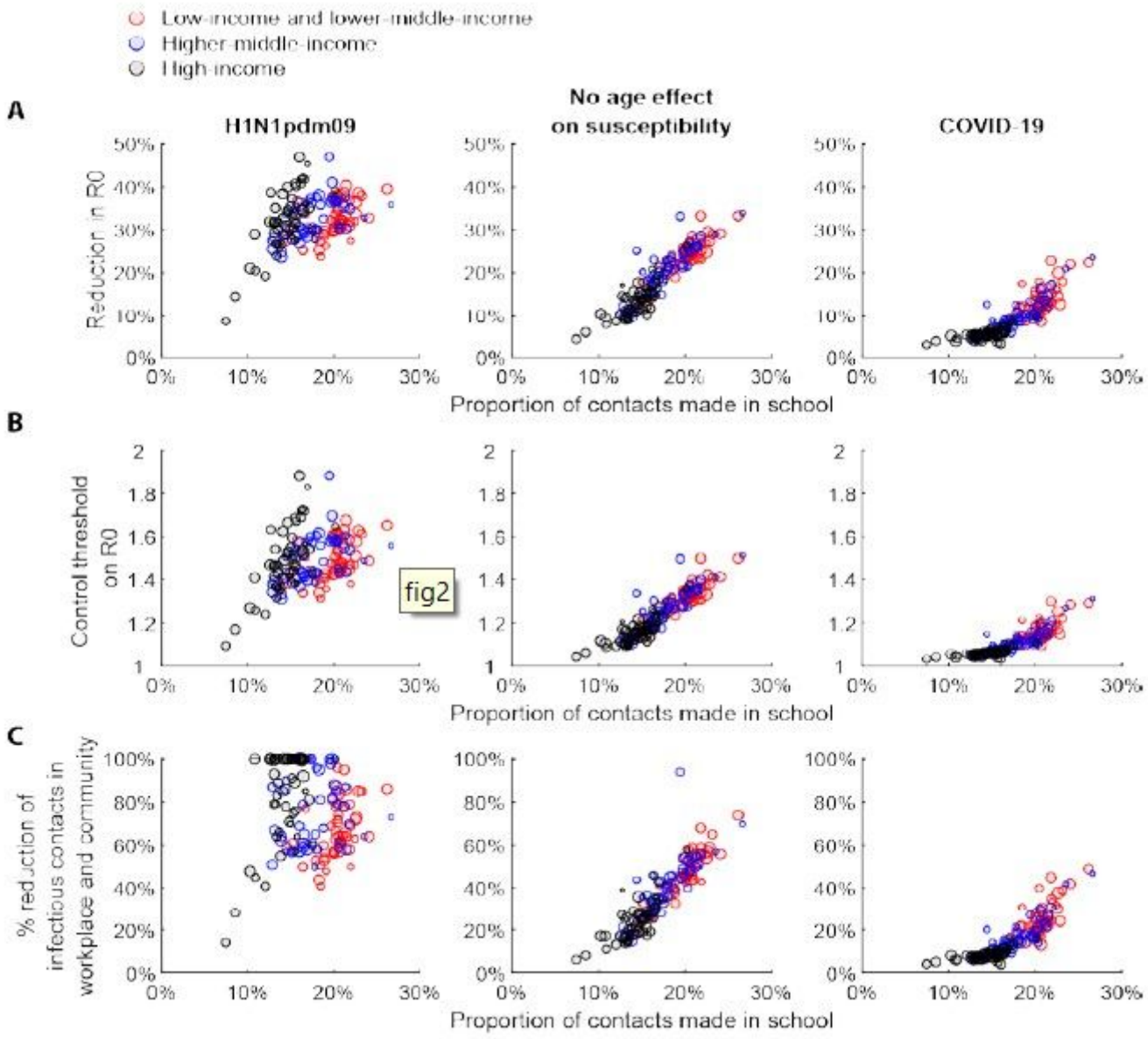


## Figure 2

The effectiveness of school closure in reducing transmissibility as a function of proportion of contacts made in school across 152 jurisdictions. See Table S1 for the numerical values of all data points shown here. The sizes of data points are proportional to the log of the corresponding population size. A Reduction in R0 conferred by school closure against H1N1pdm09 (left), a pathogen to which individual of all ages were equally susceptible (middle) and COVID-19 (right). B Outbreak threshold (in terms of R0) under school closure. C Percent reduction in workplace and community contacts that would be required in order to achieve the reduction in R0 conferred by school closure. A required percentage of 100% (for some

high-income and upper-middle-income populations in the case of H1N1pdm09) means that this was impossible.

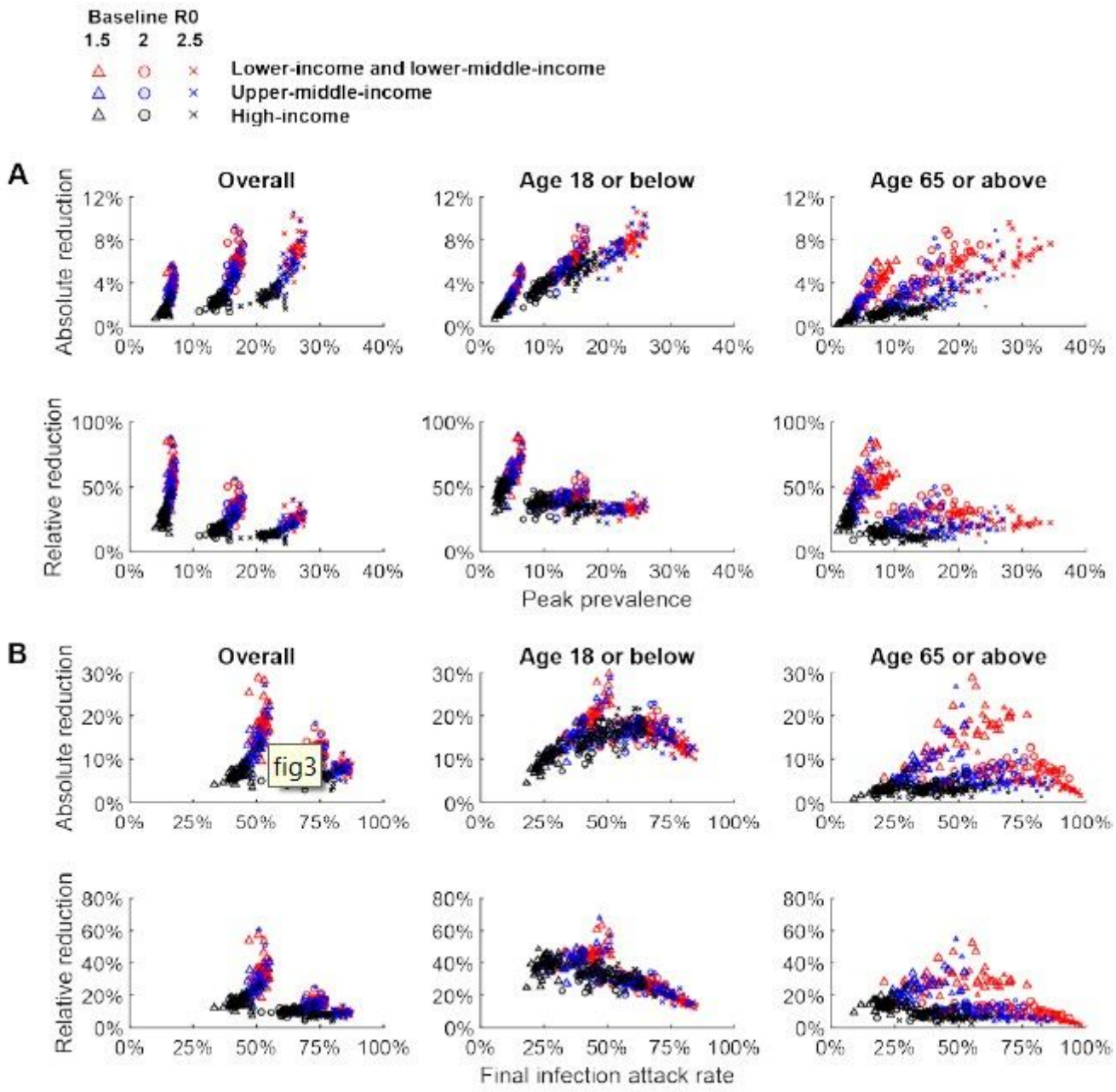


**Figure 3**

The public health impact of school closure across 152 jurisdictions. See Table S1 for the numerical values of all data points shown here. A Reduction in peak prevalence for all ages (left), those aged 18 or below (middle) and those aged 65 or above (right). B Reduction in final IAR for all ages (left), those aged 18 or below (middle) and those aged 65 or above (right).

# Supplementary Files

This is a list of supplementary files associated with this preprint. Click to download.

- schoolclosuresuppinfoTableS1.xlsx
- TableS2final.jpg
- FigureS1.jpg
- FigureS2.jpg
- FigureS3.jpg
- FigureS4.jpg
- FigureS5.jpg
- FigureS6.jpg
- FigureS7.jpg
- FigureS8.jpg
- FigureS9.jpg
- FigureS10.jpg
- FigureS11.jpg
- FigureS12.jpg
- FigureS13.jpg
- schoolclosuresuppinfo5.pdf